Letter

Preparation of High Vibrational States in the Entire Molecular Beam

Qian-Hao Liu, Hanhui Zhang, Liping Wen, Yurun Xie, Tiangang Yang,* Cun-Feng Cheng,* Shui-Ming Hu, and Xueming Yang

Cite This: *J. Phys. Chem. Lett.* 2024, 15, 9926−9931

Read Online

ACCESS | Metrics & More | Article Recommendations | SI Supporting Information

ABSTRACT: Preparing highly excited molecules is of great interest in chemistry, but it has long been a challenge due to the high laser power required within the narrow line width to excite a weak transition. We present a cavity-enhanced infrared excitation scheme using a milliwatt laser. As a demonstration, about 35% of CO molecules in a ground-state rotational level were excited to the highly excited $v = 3$ state in the entire pulsed supersonic beam, as confirmed by the depletion of molecules in the ground state. The method was also applied to excite HD molecules to the $v = 2$ state with a continuous-wave diode laser. This work provides a universal approach to prepare molecules in a specific quantum state, paving the way to study the chemical reaction dynamics of highly excited molecules.
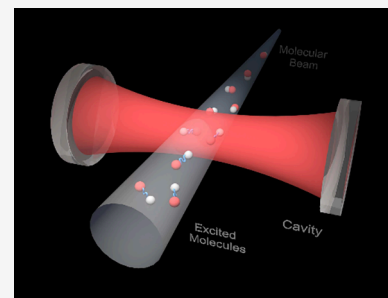
Efficient state-selective excitation of molecules is essential for state-to-state reaction dynamics experiments and the elucidation of complex reaction mechanisms.[1−6] Pumping reactants into selected rovibrational states is crucial to address core scientific theories, such as the Polanyi rules, and to perform in-depth studies of quantum effects in key reactions.[7−14] In particular, the excitation of molecules to higher rovibrational states stands at the forefront of current research, providing insight into unique reaction dynamics not observable at lower energy levels. For example, excitation to high vibrational levels allows us to discover reaction resonances caused by bond softening due to anharmonicity,[15−17] potentially expanding our scope for observing reactive resonances across a wider range of reactions. Furthermore, in gas-surface scattering experiments, overtone excitation helps to investigate nonadiabatic effect and understand the process of vibrational relaxation on surfaces.[18−23] Therefore, the drive to deeply understand chemical reaction dynamics in areas not yet explored has spurred the development of an effective overtone excitation technique in a beam.[24]

Various optical techniques, such as stimulated emission pumping (SEP),[25−28] Raman pumping,[29−32] and infrared pumping,[18,20,21,33−35] have been used for this purpose. However, the transfer of large populations to a desired higher quantum state often encounters significant difficulties. For example, SEP typically requires a VUV laser for pumping to the electronic state, resulting in successful high vibrational excitation only for a few molecules. Additionally, the transfer efficiency of SEP is generally limited to about 30% and often distributes populations to unintended levels. Stark-induced adiabatic Raman passage (SARP)[30−32] can transfer nearly the entire population between two quantum states, but it typically requires two tightly focused pulsed lasers with high field strength to induce a sufficient Stark shift. Due to the small

cross-section of the Raman effect, this approach can only excite a small fraction of the molecular beam.

Infrared laser excitation offers a simpler alternative. Basically, when molecules interact with infrared light in a nonadiabatic scheme, the population of molecules in the excited (vibrational) state within the two-level system can be expressed as

$$\frac{n^*}{n_0} = \frac{s}{2(1 + s)} \tag{1}$$

where n^* and n_0 are the number of excited molecules and the total number of molecules, respectively, $s = I/I_s$ is the saturation parameter, I and I_s denote the laser and the saturation power intensities. The saturation power intensity can be calculated with the formula $I_s = \frac{ch}{3} \frac{\Gamma^2 k^3}{A}$ given in refs 36 and 37, which is usually very large for overtone transitions. For example, it is 74 kW/cm² for the $(v = 3, j = 2) \leftarrow (v = 0, j = 1)$ transition of CO. Therefore, it is very challenging to prepare molecules in high vibrational states with direct IR excitation.

Nanosecond pulsed lasers with peak powers exceeding 100 kW/cm² have been used to excite infrared transitions, as demonstrated in the preparation of vibrationally excited CO ($v = 2$)[20,33] and NO ($v = 2, 3$).[18,21] However, given the microsecond duration of the pulsed molecular beam, only a small fraction of the beam could be excited by the pulsed laser. The complete excitation of the molecular beam is crucial in
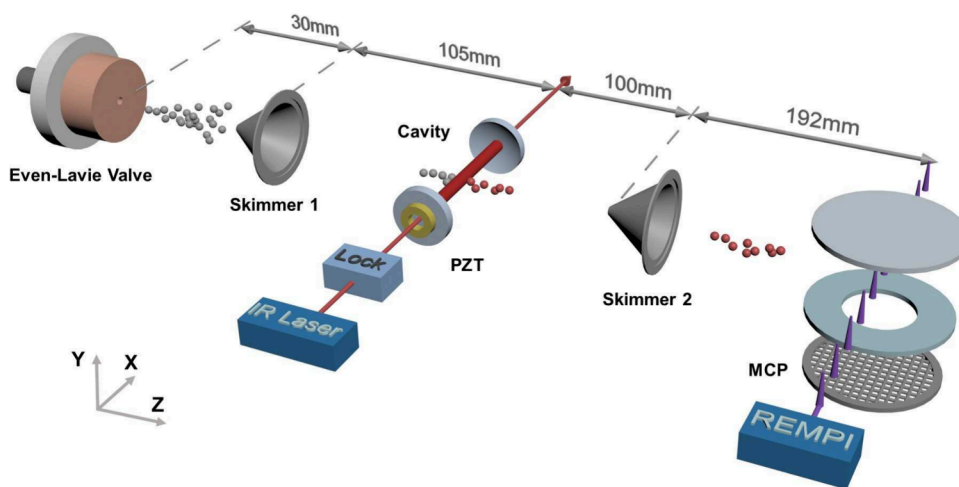
Figure 1. Schematic of the excitation experiment. Lock: Pound-Drever-Hall Locking servo; MCP: microchannel plate; PZT: piezo actuator; REMPI: laser used for resonance-enhanced multiphoton ionization.

certain experiments. For example, in surface scattering experiments,[18−23] the entire pulse of the beam interacts with a stationary surface and contributes to the overall yield. Similarly, in ion−molecule reactions[38−41] and certain scattering experiments,[42−46] the interaction region often exceeds the detection laser spot, requiring excitation of a large beam segment.

A continuous-wave (cw) laser can cover the entire pulse of the molecular beam, but the excitation efficiency is often limited by the laser power. Using a single mode cw optical parametric oscillator (OPO) system, preparation of intense molecular beams of vibration fundamental quantum-states has been realized for gas/surface reaction dynamics experiments,[12,14] even with 100% efficiency via rapid adiabatic passage process.[11,47,48] A high-finesse cavity can tremendously enhance the power of a narrow-line width cw laser, and the technique has been successfully applied to saturate overtone transitions of molecules.[49,50] Here, we propose a cavity-locked laser excitation method to prepare molecules in highly excited rovibrational states. As a demonstration, CO molecules were pumped to the ($v = 3$, $j = 1, 2$) levels, and the population transfer efficiency was determined.

A schematic setup of the experiment is shown in Figure 1. It can be divided into three parts: the molecular beam source, the IR laser and excitation cavity, and the REMPI (Resonance-Enhanced Multiphoton Ionization) detection. The molecular beam is generated by an Even-Lavie valve with a back pressure of 1 MPa to maximize the molecular number density and suppress the formation of CO clusters. The velocity of the CO beam has been measured to be 780 m/s, with a rotational temperature of about 4.5 K, corresponding to 44% of the molecules in the ($v = 0$, $j = 1$) state. Two 1 mm-diameter skimmers, 205 mm apart, are placed downstream of the molecular beam. A 6 cm-long high-finesse ($F \approx 415000$) cavity is placed between the two skimmers. The cavity consists of two low-loss (≈ 2.3 ppm) high-reflectivity ($R \approx 99.999\%$ at 1500−1600 nm) mirrors with a curvature of about 100 cm, resulting in an intracavity Gaussian full width at half-maximum of 0.6 mm. A cw external cavity diode laser (ECDL) delivers a beam with a few tens of milliwatts into the cavity. The laser frequency is locked with a cavity mode (mode width ∼6 kHz) by the Pound-Drever-Hall (PDH) method.[51] When the infrared laser (IR) is locked with the cavity and also in

resonance with the molecular transition, molecules passing through the cavity are excited by the laser. A (2 + 1) REMPI scheme is used to detect molecules after the second skimmer.

The ECDL laser frequency is also locked to a reference laser by a beat-locking servo referenced to a microwave (MW) source. In the experiment, we can either fix the MW frequency to observe the molecular excitation for a specific IR frequency, or scan the MW frequency to sweep the IR frequency to characterize the molecular beam. The laser locking scheme is similar to that described in ref.,[36] and the details are described in Supporting Information Sec 1.

To reduce vibration noise and keep the laser well locked to the optical cavity, we implement passive vibration damping to hold the main vacuum chamber and isolate the turbo pump from the chamber with bellows. It is worth noting that when the molecular beam with a duration of about 100 μs passes the optical cavity, there would be a considerable change in the refractive index. The locking servo must quickly follow the change, otherwise, no IR laser power can be injected into the cavity and the molecules cannot be excited.

First, we fixed the 2 + 1 REMPI frequency on-resonance with the E$^1\Pi$ ($v = 0$, $j = 3$) ← X$^1\Sigma^+$ ($v = 0$, $j = 1$) transition (107.6 nm) to detect the molecules and scanned the IR laser frequency around the X$^1\Sigma^+$ ($v = 3$, $j = 2$) ← ($v = 0$, $j = 1$) transition (1573 nm) to excite the molecules vibrationally, as shown in Figure 2 (A). The geometrical relationship of the excitation laser and the transverse number density distribution of molecules in the vibrationally excited states (red shadow) in the detection zone are shown schematically in Figure 2 (B). The pre-cavity IR power was 21 mW, corresponding to an intracavity power intensity of 750 kW/cm^2 and a saturation parameter $s = 10$ under a calculated transit-time broadening[37,52] of about 1.0 MHz. When we scanned the excitation IR frequency, we obtained a depletion spectrum as illustrated in Figure 2 (C). The signal could be well fitted with a Gaussian function, with the amplitude indicating a maximum depletion of 35%. The width of the dip was about 6 MHz, indicating the Doppler broadening convoluted with the transit-time broadening and power broadening. From the spectrum of scanning the IR laser frequency, we confirmed that the best excitation efficiency appears when the long-term frequency drift is controlled to be less than 1 MHz.
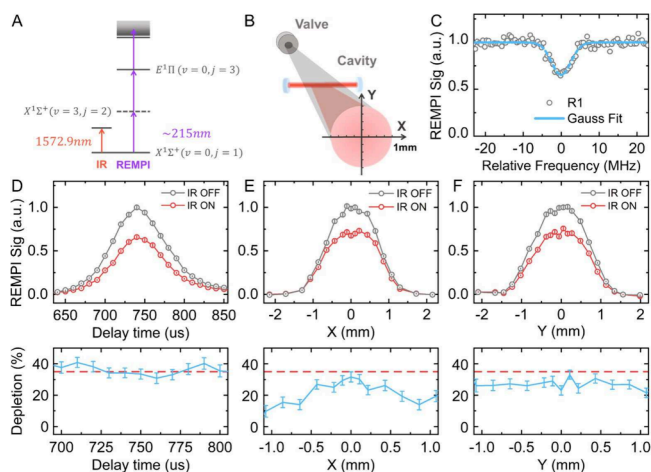
Figure 2. (A) Energy levels of CO and the depletion scheme of the experiment. (B) The schematic drawing of the geometrical relation of the excitation laser and the transverse number density distribution of molecules in the vibrationally excited (red shadow) states. (C) The REMPI depletion spectrum obtained by scanning the IR laser frequency. (D) The TOF signal of the molecular beam with the IR ON (red) and OFF (black). Note that the x-axis of the graph is expressed with the speed of the molecular beam multiplied by the delay time. (E) The REMPI signal when scanning the position of the REMPI laser beam along the X-axis with the IR ON (red) and OFF (black). (F) The REMPI signal when scanning the position of the REMPI laser beam along the Y-axis with the IR ON (red) and OFF (black). Data in (D), (E), and (F) were measured with the IR frequency locked on-resonance with the $(v = 3, j = 2) \leftarrow (v = 0, j = 1)$ transition, and the lower panels show the corresponding depletion signal. The red dashed lines in (D), (E), and (F) indicate population transfer efficiency of 35%, corresponding to the on-resonance population transfer efficiency shown in (C).

Then we fixed the IR laser frequency at the center of the $(v = 3, j = 2) \leftarrow (v = 0, j = 1)$ transition and obtained a time-of-flight (TOF) signal, shown in Figure 2(D), with the IR on (red) and off (black). As shown in the figure, the pulse width of the molecular beam was about 80 μs. The bottom panel of Figure 2(D) shows the depletion, calculated with $1 -$ Signal (IR ON)/Signal (IR OFF), and the red dashed line indicates the depletion value of 35% averaged over the pulse duration of about 100 μs. The result shows that the depletion ratio was almost the same throughout the pulse. Note that the arrival of the molecular beam pulse could change the refractive index inside the optical cavity, which was observed from the error signal of the cavity locking servo, but the servo can quickly follow the change and maintain the lock.

We also observed the spatial distribution of the depletion effect induced by the IR excitation. While keeping both IR and REMPI lasers in resonance, we actively changed the position of the REMPI laser beam along the X- and Y-axes, and the results are shown in Figures 2(E) and (F), respectively. The depletion signal remains about 20−30% within the whole molecular beam with a radius of about 1 mm. Note that the distributions along the X-axis and Y-axis are different. The IR laser propagates along the X-axis, and the transit-time broadening limits the transverse velocities of molecules that can interact with the IR beam. In the Y-axis, the size of the IR laser beam dominates the interaction range. The detailed calculation of the area occupied by the excited molecules is given in the Supporting Information Sec 2. The averaged population

transfer efficiency is estimated to be 24.4% within the part with a 2 mm diameter portion of the molecular beam.

We have also demonstrated the selective excitation of molecules into different rovibrational states. Figure 3 shows the
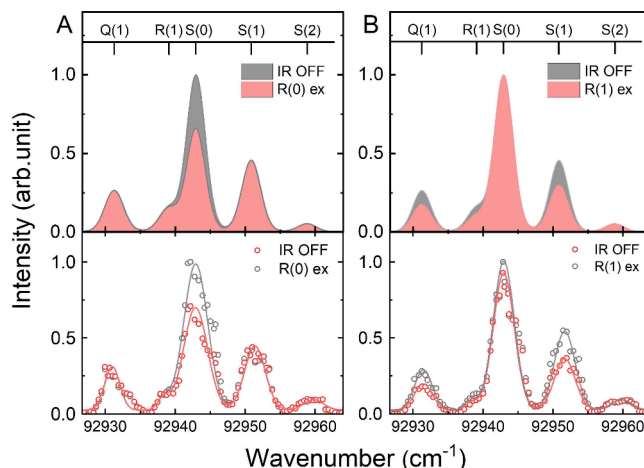

Figure 3. REMPI spectra of the ground vibrational state of CO. The PGOPHER simulated spectra are presented in the upper panel, and the experimental spectra are shown in the lower panel. Gray and red shadow/dots indicate the signal with the IR light off and on, respectively. (A) R(0) ex: the IR laser was on-resonance with the $(v = 3, j = 1) \leftarrow (v = 0, j = 0)$ line. (B) R(1) ex: the IR laser was on-resonance with the $(v = 3, j = 2) \leftarrow (v = 0, j = 1)$ line.

results of IR excitation through the R(0) $(v = 3, j = 1) \leftarrow (v = 0, j = 0)$ and R(1) $(v = 3, j = 2) \leftarrow (v = 0, j = 1)$ transitions, respectively. The top panels are the REMPI spectra simulated by PGOPHER and the bottom panels are the experimental results. The IR excitation inherits the high resolution of the CW laser. Consequently, when a selected quantum state is excited, the others are not affected. The population transfer efficiency is confirmed to be about 35% for both R(0) and R(1) transitions, agreeing with the depletion measurements.

This method is essentially based on infrared transitions and is applicable to all infrared active molecules, such as CO_2, H_2O, NH_3, CH_4, etc. As a special example, HD molecules in the $(v = 2, j = 1)$ state are excited by the overtone transition of $(v = 2, j = 1) \leftarrow (v = 0, j = 0)$ near 1395 nm. The HD transition is extremely weak, with an Einstein-A coefficient of 2×10^{-5} s^{-1},[53] and the saturation power intensity reaches 0.11 GW/cm^2. We achieved an intracavity IR laser power intensity of 2.6 MW/cm^2 using a fiber laser with 800 mW and transferred about 1.2% of HD molecules from the $(v = 0, j = 0)$ state to the $(v = 2, J = 1)$ state. The REMPI spectrum of the excited HD molecules is shown in Figure 4 (A). Figure 4 (B) shows the TOF signal of the excited HD molecules, indicating that the excitation affected the HD molecules in the entire beam. Note that the infrared excitation efficiency is strongly dependent on the intracavity laser power intensity. The calculated dependence is shown in Figure 4 (C), with the result demonstrated in this work marked with the red dot. By using mirrors with a better coating[54−56] and a more powerful fiber amplifier, we expect a significant improvement in the near future.

We developed a cavity-enhanced IR pumping method based on continuous-wave lasers to generate a vibrationally excited molecular beam. By locking a milliwatt diode laser into a high-finesse cavity, we demonstrated an intracavity laser power
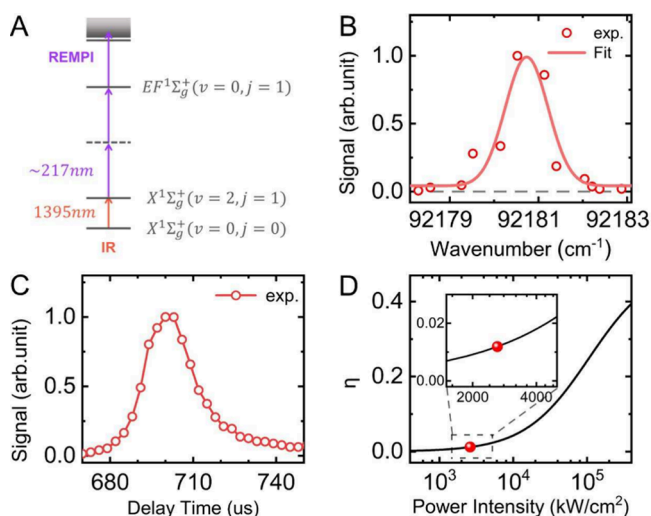
Figure 4. (A) Energy levels of HD and the excitation/ionization scheme in the experiment. (B) The REMPI spectrum of the $X^1\Sigma_g^+$ ($v = 2$, $j = 1$) state of HD (red dot), the Gaussian fitting (red line), compared with the baseline without IR excitation (gray dash). (C) The TOF signal of the vibrationally excited HD molecules (red dotted-line, $X^1\Sigma_g^+$ ($v = 2$, $j = 1$)). (D) The calculated population transfer efficiency (η) related to the intracavity laser power intensity. The red point represents the current experimental condition.

intensity of 750 kW/cm², which excited carbon monoxide molecules in a pulsed beam to the $v = 3$ state through rovibrational transitions from the ground state. The temporal and spatial distribution of the excited molecules in the beam was analyzed by resonance-enhanced multiphoton ionization spectroscopy, indicating an excitation efficiency up to 35% throughout the molecular beam. Compared to other methods, the one presented in this work has some remarkable advantages. The first is that the enhancement due to the high-finesse cavity allows excitation by weak transitions. As shown in the excitation of HD molecules to the $v = 2$ state, the infrared transition of HD is extremely weak, characterized by an Einstein A-coefficient approximately 6 orders of magnitude smaller than that of a typical fundamental transition of CO. This advantage allows us to excite molecules to very high vibrational states, with energies exceeding 0.8 eV, that are inaccessible by other methods. The second advantage is the use of continuous-wave lasers instead of pulsed lasers. With proper geometrical alignment of the excitation cavity and the molecular beam, one can excite molecules in the entire beam instead of just a small portion in space/time. This is particularly advantageous when the entire beam contributes to the experimental signal. In addition, since the excitation uses relatively simple dipole transitions, the excitation efficiency can be easily quantified, which is essential for many quantitative studies.

The presented approach paves the way for a number of important fundamental studies and applications. It provides an opportunity to study the dynamics of state-selected molecular reactions, especially when the vibrational excited states are needed, to search for novel quantum effects in chemical reactions and reveal the quantum nature of chemical reactions.[57,58] Moreover, the significant change in the population of quantum states enables coherent measurements, such as Ramsey spectroscopy[59] of molecular vibrational transitions, leading to the development of molecular interferometers, which will greatly improve the precision measurements of molecules.[60−62] Since the infrared transitions are distinguishable for different molecular isotopologues, this method can also be applied to study isotopic effects such as isotope separation and enrichment.[63,64]

■ ASSOCIATED CONTENT

Ⓢ Supporting Information

The Supporting Information is available free of charge at https://pubs.acs.org/doi/10.1021/acs.jpclett.4c02396.

Additional details of the experiment and data analysis, including the frequency locking approach (shown with Figure S1 and text) and the simulation of the molecular population transfer efficiency (shown with Figure S2 and text) (PDF)

■ AUTHOR INFORMATION

Corresponding Authors

Tiangang Yang − *Department of Chemistry, and Center for Advanced Light Source, Southern University of Science and Technology, Shenzhen 518055, China;* Ⓞ orcid.org/0000-0002-8940-8875; Email: yangtg@sustech.edu.cn

Cun-Feng Cheng − *State Key Laboratory of Molecular Reaction Dynamics, Department of Chemical Physics, University of Science and Technology of China, Hefei 230026, China; Hefei National Research Center of Physical Sciences at the Microscale, University of Science and Technology of China, Hefei 230026, China; Hefei National Laboratory, University of Science and Technology of China, Hefei 230088, China;* Ⓞ orcid.org/0000-0003-3637-0989; Email: cfcheng@ustc.edu.cn

Authors

Qian-Hao Liu − *State Key Laboratory of Molecular Reaction Dynamics, Department of Chemical Physics, University of Science and Technology of China, Hefei 230026, China*

Hanhui Zhang − *Institute of Advanced Science Facilities, Shenzhen 518107, China*

Liping Wen − *Department of Chemistry, and Center for Advanced Light Source, Southern University of Science and Technology, Shenzhen 518055, China;* Ⓞ orcid.org/0009-0006-2589-8365

Yurun Xie − *Department of Chemistry, and Center for Advanced Light Source, Southern University of Science and Technology, Shenzhen 518055, China; Institute of Advanced Science Facilities, Shenzhen 518107, China*

Shui-Ming Hu − *State Key Laboratory of Molecular Reaction Dynamics, Department of Chemical Physics, University of Science and Technology of China, Hefei 230026, China; Hefei National Laboratory, University of Science and Technology of China, Hefei 230088, China;* Ⓞ orcid.org/0000-0002-1565-8468

Xueming Yang − *Department of Chemistry, and Center for Advanced Light Source, Southern University of Science and Technology, Shenzhen 518055, China; Hefei National Laboratory, University of Science and Technology of China, Hefei 230088, China; State Key Laboratory of Molecular Reaction Dynamics, Dalian Institute of Chemical Physics, Chinese Academy of Science, Dalian 116023, China*

Complete contact information is available at:
https://pubs.acs.org/10.1021/acs.jpclett.4c02396

■ REFERENCES

(1) Neuhauser, D.; Judson, R.; Kouri, D.; Adelman, D.; Shafer, N.; Kliner, D.; Zare, R. State-to-state rates for the D + $H_2(v = 1, j = 1) \rightarrow$ HD(v', j') + H reaction: predictions and measurements. *Science* 1992, *257*, 519−522.

(2) Kitsopoulos, T.; Buntine, M.; Baldwin, D.; Zare, R.; Chandler, D. Reaction product imaging: the H + D_2 reaction. *Science* 1993, *260*, 1605−1610.

(3) Segev, Y.; Bibelnik, N.; Akerman, N.; Shagam, Y.; Luski, A.; Karpov, M.; Narevicius, J.; Narevicius, E. Molecular beam brightening by shock-wave suppression. *Science Advances* 2017, *3* (No), No. e1602258.

(4) Schnieder, L.; Seekamprahn, K.; Borkowski, J.; Wrede, E.; Welge, K.; Aoiz, F.; Banares, L.; Dmello, M.; Herrero, V.; Rabanos, V.; Wyatt, R. Experimental studies and theoretical predictions for the H + $D_2 \rightarrow$ HD + D reaction. *Science* 1995, *269*, 207−210.

(5) Harich, S.; Dai, D.; Wang, C.; Yang, X.; Chao, S.; Skodje, R. Forward scattering due to slow-down of the intermediate in the H + HD → D + H_2 reaction. *Nature* 2002, *419*, 281−284.

(6) Tang, G.; Besemer, M.; Kuijpers, S.; Groenenboom, G. C.; van der Avoird, A.; Karman, T.; van de Meerakker, S. Y. T. Quantum state-resolved molecular dipolar collisions over four decades of energy. *Science* 2023, *379*, 1031−1036.

(7) Zhang, W.; Kawamata, H.; Liu, K. CH stretching excitation in the early barrier F + CHD_3 reaction inhibits CH bond cleavage. *Science* 2009, *325*, 303−306.

(8) Yan, S.; Wu, Y.-T.; Zhang, B.; Yue, X.-F.; Liu, K. Do vibrational excitations of CHD_3 preferentially promote reactivity toward the chlorine atom? *Science* 2007, *316*, 1723−1726.

(9) Wang, F.; Lin, J.-S.; Liu, K. Steric control of the reaction of CH stretch-excited CHD_3 with chlorine atom. *Science* 2011, *331*, 900−903.

(10) Wang, T.; Chen, J.; Yang, T.; Xiao, C.; Sun, Z.; Huang, L.; Dai, D.; Yang, X.; Zhang, D. H. Dynamical resonances accessible only by reagent vibrational excitation in the F + HD → HF + D reaction. *Science* 2013, *342*, 1499−1502.

(11) Pan, H.; Mondal, S.; Yang, C.-H.; Liu, K. Imaging characterization of the rapid adiabatic passage in a source-rotatable, crossed-beam scattering experiment. *J. Chem. Phys.* 2017, *147*, 013928.

(12) Yoder, B. L.; Bisson, R.; Beck, R. D. Steric effects in the chemisorption of vibrationally excited methane on Ni(100). *Science* 2010, *329*, 553−556.

(13) Hundt, P. M.; Jiang, B.; van Reijzen, M. E.; Guo, H.; Beck, R. D. Vibrationally promoted dissociation of water on Ni(111). *Science* 2014, *344*, 504−507.

(14) Pan, H.; Liu, K. Fermi-phase-induced interference in the reaction between Cl and vibrationally excited CH_3D. *Nat. Chem.* 2022, *14*, 545−549.

(15) Xu, X.; Liu, S.; Chen, J.; Zhang, D. H. High vibrational excitation of the reagent transforms the late-barrier H + HOD reaction into an early-barrier reaction. *J. Chem. Phys.* 2024, *160*, 041101.

(16) Liu, S.; Zhang, X.; Chen, J.; Zhang, D. H. Feshbach resonances in the vibrationally excited F + HOD (v_{OH}/v_{OD}=1) reaction due to chemical bond softening. *J. Phys. Chem. Lett.* 2021, *12*, 6090−6094.

(17) Yang, T.; Chen, J.; Huang, L.; Wang, T.; Xiao, C.; Sun, Z.; Dai, D.; Yang, X.; Zhang, D. H. Extremely short-lived reaction resonances in Cl + HD (v = 1) → DCl + H due to chemical bond softening. *Science* 2015, *347*, 60−63.

(18) Golibrzuch, K.; Shirhatti, P. R.; Rahinov, I.; Auerbach, D. J.; Wodtke, A. M.; Bartels, C. Incidence energy dependent state-to-state time-of-flight measurements of NO(v = 3) collisions with Au(111): the fate of incidence vibrational and translational energy. *Phys. Chem. Chem. Phys.* 2014, *16*, 7602−7610.

(19) Bartels, N.; Golibrzuch, K.; Bartels, C.; Chen, L.; Auerbach, D. J.; Wodtke, A. M.; Schaefer, T. Dynamical steering in an electron transfer surface reaction: oriented NO(v = 3, 0.08< Ei < 0.89 eV) relaxation in collisions with a Au(111) surface. *J. Chem. Phys.* 2014, *140*, 54710.

(20) Shirhatti, P. R.; Rahinov, I.; Golibrzuch, K.; Werdecker, J.; Geweke, J.; Altschaeffel, J.; Kumar, S.; Auerbach, D. J.; Bartels, C.; Wodtke, A. M. Observation of the adsorption and desorption of vibrationally excited molecules on a metal surface. *Nat. Chem.* 2018, *10*, 592−598.

(21) Golibrzuch, K.; Shirhatti, P. R.; Altschaeffel, J.; Rahinov, I.; Auerbach, D. J.; Wodtke, A. M.; Bartels, C. State-to-state time-of-flight measurements of NO scattering from Au(111): direct observation of translation-to-vibration coupling in electronically nonadiabatic energy transfer. *J. Phys. Chem. A* 2013, *117*, 8750−8760.

(22) Cooper, R.; Bartels, C.; Kandratsenka, A.; Rahinov, I.; Shenvi, N.; Golibrzuch, K.; Li, Z.; Auerbach, D. J.; Tully, J. C.; Wodtke, A. M. Multiquantum vibrational excitation of NO scattered from Au(111): quantitative comparison of benchmark data to ab initio theories of nonadiabatic molecule-surface interactions. *Angew. Chem., Int. Ed.* 2012, *51*, 4954−4958.

(23) Shirhatti, P.; Werdecker, J.; Golibrzuch, K.; Wodtke, A.; Bartels, C. Electron hole pair mediated vibrational excitation in CO scattering from Au(111): Incidence energy and surface temperature dependence. *J. Chem. Phys.* 2014, *141*, 124704.

(24) Bergmann, K.; Vitanov, N. V.; Shore, B. W. Perspective: stimulated raman adiabatic passage: the status after 25 years. *J. Chem. Phys.* 2015, *142*, 170901.

(25) Geers, A.; Kappert, J.; Temps, F.; Wiebrecht, J. State-selective vibrational-excitation of OH ($X^2\Pi$) radicals by stimulated-emission pumping. *Chem. Phys. Lett.* 1989, *155*, 614−619.

(26) Yang, X.; Wodtke, A. Efficient state-specific preparation of highly vibrationally excited NO ($X^2\Pi$). *J. Chem. Phys.* 1990, *92*, 116−120.

(27) Lambert, H.; Carrington, T.; Filseth, S.; Sadowski, C. Single rotational state preparation and relaxation in CN ($X^2\Sigma$,v = 2)-stimulated-emission pumping and laser-induced fluorescence detection. *Chem. Phys. Lett.* 1990, *169*, 185−190.

(28) Bartels, N.; Krueger, B. C.; Meyer, S.; Wodtke, A. M.; Schaefer, T. Suppression of spontaneous emission in the optical pumping of molecules: pump-dump-sweep-probe. *J. Phys. Chem. Lett.* 2013, *4*, 2367−2370.

(29) Yang, T.-G.; Huang, L.; Wang, T.; Xiao, C.-L.; Dai, D.-X.; Yang, X.-M. Efficient preparation of D_2 Molecules in v = 2 by stimulated raman pumping. *Chin. J. Chem. Phys.* **2017**, *30*, 614−618.

(30) Perreault, W. E.; Mukherjee, N.; Zare, R. N. Preparation of a selected high vibrational energy level of isolated molecules. *J. Chem. Phys.* **2016**, *145*, 154203.

(31) Perreault, W. E.; Zhou, H.; Mukherjee, N.; Zare, R. N. Harnessing the power of adiabatic curve crossing to populate the highly vibrationally excited H_2 (v = 7, j = 0) level. *Phys. Rev. Lett.* **2020**, *124*, 163202.

(32) Mukherjee, N.; Perreault, W. E.; Zare, R. N. Stark-induced adiabatic raman ladder for preparing highly vibrationally excited quantum states of molecular hydrogen. *J. Phys. B: At. Mol. Opt. Phys.* **2017**, *50*, 144005.

(33) Kumar, A.; Singh, S. K.; Shirhatti, P. R. A versatile and narrow linewidth infrared radiation source for ro-vibration state-selected preparation of molecules in molecular beams. *Rev. Sci. Instrum.* **2023**, *94*, 113001.

(34) Korolik, M.; Suchan, M.; Johnson, M.; Arnold, D.; Reisler, H.; Wittig, C. Survival of HCl(v = 2) in trapping-desorption from MgO(100). *Chem. Phys. Lett.* **2000**, *326*, 11−21.

(35) Rahinov, I.; Cooper, R.; Yuan, C.; Yang, X.; Auerbach, D. J.; Wodtke, A. M. Efficient vibrational and translational excitations of a solid metal surface: state-to-state time-of-flight measurements of HCl(v = 2,J = 1) scattering from Au(111). *J. Chem. Phys.* **2008**, *129*, 214708.

(36) Wang, J.; Sun, Y. R.; Tao, L.-G.; Liu, A.-W.; Hu, S.-M. Communication: molecular near-infrared transitions determined with sub-kHz accuracy. *J. Chem. Phys.* **2017**, *147*, 091103.

(37) Demtröder, W. *Laser spectroscopy: Vol. 1: Basic Principles*, 4th ed.; Springer-Verlag; 2008; Chapter 3, pp 85−88; 978-3-662-49542-1.

(38) Yang, T.; Li, A.; Chen, G. K.; Xie, C.; Suits, A. G.; Campbell, W. C.; Guo, H.; Hudson, E. R. Optical control of reactions between water and laser-cooled Be^+ ions. *J. Phys. Chem. Lett.* **2018**, *9*, 3555−3560.

(39) Yang, T.; Li, A.; Chen, G. K.; Yao, Q.; Suits, A. G.; Guo, H.; Hudson, E. R.; Campbell, W. C. Isomer-specific kinetics of the C^+ + H_2O reaction at the temperature of interstellar clouds. *Science Advances* **2021**, *7*, No. eabe4080.

(40) Tong, X.; Nagy, T.; Reyes, J. Y.; Germann, M.; Meuwly, M.; Willitsch, S. State-selected ion−molecule reactions with coulomb-crystallized molecular ions in traps. *Chem. Phys. Lett.* **2012**, *547*, 1−8.

(41) Willitsch, S.; Bell, M. T.; Gingell, A. D.; Procter, S. R.; Softley, T. P. Cold reactive collisions between laser-cooled ions and velocity-selected neutral molecules. *Phys. Rev. Lett.* **2008**, *100*, 043203.

(42) Carrascosa, E.; Meyer, J.; Wester, R. Imaging the dynamics of ion−molecule reactions. *Chem. Soc. Rev.* **2017**, *46*, 7498−7516.

(43) Margulis, B.; Horn, K. P.; Reich, D. M.; Upadhyay, M.; Kahn, N.; Christianen, A.; van der Avoird, A.; Groenenboom, G. C.; Koch, C. P.; Meuwly, M.; Narevicius, E. Tomography of feshbach resonance states. *Science* **2023**, *380*, 77−81.

(44) Gordon, S. D. S.; Omiste, J. J.; Zou, J.; Tanteri, S.; Brumer, P.; Osterwalder, A. Quantum-state-controlled channel branching in cold Ne($^3P_2$)+ Ar chemi-ionization. *Nat. Chem.* **2018**, *10*, 1190−1195.

(45) Heazlewood, B. R.; Softley, T. P. Towards chemistry at absolute zero. *Nature Reviews Chemistry* **2021**, *5*, 125−140.

(46) Jankunas, J.; Osterwalder, A. Cold and controlled molecular beams: production and applications. *Annu. Rev. Phys. Chem.* **2015**, *66* (1), 241−262.

(47) Liedenbaum, C.; Stolte, S.; Reuss, J. Inversion produced and reversed by adiabatic passage. *Physics Reports-Review Section of Physics Letters* **1989**, *178*, 1−24.

(48) Chadwick, H.; Hundt, P. M.; van Reijzen, M. E.; Yoder, B. L.; Beck, R. D. Quantum state specific reactant preparation in a molecular beam by rapid adiabatic passage. *J. Chem. Phys.* **2014**, *140*, 034321.

(49) Hu, C.-L.; Perevalov, V.; Cheng, C.-F.; Hua, T.-P.; Liu, A.-W.; Sun, Y. R.; Tan, Y.; Wang, J.; Hu, S.-M. Optical-optical double-resonance absorption spectroscopy of molecules with kilohertz accuracy. *J. Phys. Chem. Lett.* **2020**, *11*, 7843−7848.

(50) Hu, C.-L.; Wang, J.; Hua, T.-P.; Liu, A.-W.; Sun, Y. R.; Hu, S.-M. Comb-locked cavity-assisted double-resonance molecular spectroscopy based on diode lasers. *Rev. Sci. Instrum.* **2021**, *92*, 073003.

(51) Drever, R. W. P.; Hall, J. L.; Kowalski, F. V.; Hough, J.; Ford, G. M.; Munley, A. J.; Ward, H. Laser phase and frequency stabilization using an optical resonator. *Appl. Phys. B: Laser Opt.* **1983**, *31*, 97−105.

(52) Ma, L. S.; Ye, J.; Dubé, P.; Hall, J. L. Ultrasensitive frequency-modulation spectroscopy enhanced by a high-finesse optical cavity: theory and application to overtone transitions of C_2H_2 and C_2HD. *J. Opt. Soc. Am. B* **1999**, *16*, 2255−2268.

(53) Gordon, I. E.; Rothman, L. S.; Hill, C.; Kochanov, R. V.; Tan, Y.; Bernath, P. F.; Birk, M.; Boudon, V.; Campargue, A.; Chance, K.; et al. The HITRAN2016 molecular spectroscopic database. *J. Quant. Spectrosc. Radiat. Transfer* **2017**, *203*, 3−69.

(54) Truong, G.-W.; Perner, L. W.; Bailey, D. M.; Winkler, G.; Cataño-Lopez, S.; Wittwer, V. J.; Südmeyer, T.; Nguyen, C.; Follman, D.; Fleisher, A. J.; Heckl, O. H.; Cole, G. D. Mid-infrared supermirrors with finesse exceeding 400 000. *Nat. Commun.* **2023**, *14*, 7846.

(55) Chalermsongsak, T.; Hall, E. D.; Cole, G. D.; Follman, D.; Seifert, F.; Arai, K.; Gustafson, E. K.; Smith, J. R.; Aspelmeyer, M.; Adhikari, R. X. Coherent cancellation of photothermal noise in GaAs/$Al_{0.92}Ga_{0.08}$As bragg mirrors. *Metrologia* **2016**, *53*, 860.

(56) Jin, N.; McLemore, C. A.; Mason, D.; Hendrie, J. P.; Luo, Y.; Kelleher, M. L.; Kharel, P.; Quinlan, F.; Diddams, S. A.; Rakich, P. T. Micro-fabricated mirrors with finesse exceeding one million. *Optica* **2022**, *9*, 965−970.

(57) Guo, H. Dynamical resonances in chemical reactions. *National Science Review* **2015**, *2*, 252−253.

(58) Wang, T.; Yang, T.; Xiao, C.; Sun, Z.; Zhang, D.; Yang, X.; Weichman, M. L.; Neumark, D. M. Dynamical resonances in chemical reactions. *Chem. Soc. Rev.* **2018**, *47*, 6744−6763.

(59) Shelkovnikov, A.; Butcher, R. J.; Chardonnet, C.; Amy-Klein, A. Stability of the proton-to-electron mass ratio. *Phys. Rev. Lett.* **2008**, *100*, 150801.

(60) Cronin, A. D.; Schmiedmayer, J.; Pritchard, D. E. Optics and interferometry with atoms and molecules. *Rev. Mod. Phys.* **2009**, *81*, 1051−1129.

(61) Dörre, N.; Rodewald, J.; Geyer, P.; von Issendorff, B.; Haslinger, P.; Arndt, M. Photofragmentation beam splitters for matter-wave interferometry. *Phys. Rev. Lett.* **2014**, *113*, 233001.

(62) Cheng, C.; van der Poel, A. P. P.; Jansen, P.; Quintero-Pérez, M.; Wall, T. E.; Ubachs, W.; Bethlem, H. L. Molecular Fountain. *Phys. Rev. Lett.* **2016**, *117*, 253201.

(63) Makarov, G. N. Low energy methods of molecular laser isotope separation. *Physics-Uspekhi* **2015**, *58*, 670.

(64) Mathi, P.; Parthasarathy, V.; Nayak, A. K.; Mittal, J. P.; Sarkar, S. K. Laser isotope separation: science and technology. *Proc. Natl. Acad. Sci., India, Sect. A Phys. Sci.* **2015**, *2*, 252−253.